Partial Force Control of Constrained Floating-Base Robots

Andrea Del Prete*, Francesco Nori†, Giorgio Metta*, Lorenzo Natale*
*iCub Facility, †RBCS Department,
Istituto Italiano di Tecnologia, Genova, Italy
Email: name.surname@iit.it

***Abstract*—We present a new method to control the motion and (a subset of) the contact forces of a floating-base robot. Legged robots are typically in rigid contact with the environment at multiple locations, hence their motion is constrained by contacts. This work is based on the technique of constraint nullspace projection, which proved effective in controlling constrained underactuated robots. However, this technique does not allow to control the constraint forces, so it may fail in certain situations. For instance, every time there is a transition of the contact state (i.e. the robot makes/breaks a contact), not controlling the transient contact force could result in jerky motion. Our idea is to project the system dynamics into the nullspace of a subset of the constraints, so that the remaining constraints can be controlled. This new control law is simple and has low computational cost because it does not require the computation of the mass matrix. Simulations were carried out to achieve static walking and other behaviors using the presented approach.**

I. Introduction

The control of floating-base mechanical systems (e.g. legged robots) is challenging because these systems are *underactuated*, hence they cannot be feedback-linearized [15]. The problem becomes even more complex when these systems are *constrained*, that is their dynamics is subject to a set of (possibly time-varying) nonlinear constraints. This is the typical case for legged robots, whose motion is constrained by the rigid contacts with the ground. Rigid contacts introduce into the system dynamics the (unknown) contact forces f, which we need to estimate in order to compute the control torques τ. A possible way around this problem is to measure the contact forces f using force/torque sensors. However, force/torque measurements are noisy and introduce delay in the control action. Moreover, very few robotic platforms are equipped with enough sensors to measure contact forces on their whole body, so this approach may be unfeasible.

Sentis [14] and Park [9] tackled this problem by computing the contact forces f as a function of the robot state $(q, \dot{q})$ and the control torques τ. Substituting this expression into the system dynamics results in the *constrained dynamics*, which does not contain the constraint forces f. Using this new dynamics, they presented a control framework for prioritized motion and force control of humanoid robots.

Righetti et al. proposed an alternative approach [11] based on recent results from analytical dynamics [1]. Rather than computing f, they projected the robot dynamics into the nullspace of the constraints, using a projector that depends only on the robot geometry. The constraint forces are cancelled by the projection, so there is no need to measure them. These kinematic projectors are faster to compute than projectors containing the mass matrix of the robot, so we get simpler and more efficient control laws.

Mistry et al. [8] presented an in-between approach, extending the Operational Space formulation [7] to underactuated constrained mechanical systems. This new formulation uses kinematic projectors [1], but it is not computationally efficient because it makes use of the inverse of the robot mass matrix. Moreover, they treat underactuation as a constraint that is solved in the nullspace of the main control task, which may result in suboptimal solutions if the task is unfeasible.

Saab et al. [13] introduced inequality constraints inside the control problem to model either control tasks or physical constraints such as joint limits and motor torque bounds. The authors demonstrate how to use inequalities to account for the well-known ZMP conditions in walking. However, introducing inequalities increases the computational complexity of the optimization problem, making the implementation of the solver critical for achieving real-time performances [5].

All these approaches present two drawbacks. First, they are safe only as long as the contact geometry does not allow the robot to apply unbounded contact forces. If a robot is in contact with the ground only, the forces are limited by its weight and the contact frictions, so we can safely not control them. On the contrary, if a robot makes additional contacts, then it can apply much higher forces, which may be only limited by its motor powers. Our approach allows to solve this issue by controlling — besides the motion — the constraint forces too. Second, when a robot makes or breaks a contact, this causes a discontinuity in the constraints, which results in discontinuous control torques. These discontinuities may generate jerky movements or, even worse, make the robot slip and fall. With the presented approach, instead, we can control the transient contact forces ensuring smooth transition between the different contact states.

Inspired by optimization-based control [3], we formulate the control problem as a (cascade of) QP constrained minimization(s). However, rather than solving the problem as it is, we exploit the problem structure to find a more efficient solution.

II. Method

This section presents the derivation of an efficient law to control a subset of the contact forces exerted by a floating-base mechanical system. Afterwards we incorporate the derived control law into a prioritized multi-task motion/force control framework. Finally we show how to exploit the remaining control redundancy to optimize a quadratic function of the uncontrolled constraint forces.

A. Single Force Control Task

The state of a floating-base rigid robot with n joints can be expressed as a vector $q \in \mathbb{R}^{n+6}$, where the first 6 elements represent the position and orientation of the floating base (e.g. the hip link) and the remaining n elements represent the joint angles. Suppose that the robot is subject to a set of k nonlinear holonomic equality constraints[1]: $c(q) = 0$, which for instance could be due to a rigid contact. Its equations of motion are:

$$M(q)\ddot{q} + h(q, \dot{q}) - J_c(q)^T f = S^T \tau, \tag{1}$$

where $M \in \mathbb{R}^{n+6 \times n+6}$ is the inertia matrix, $\ddot{q} \in \mathbb{R}^{n+6}$ contains the joint accelerations and base linear/angular accelerations, $h \in \mathbb{R}^{n+6}$ are the bias forces (i.e. gravity, centrifugal and Coriolis), $S = \begin{bmatrix} 0_{n\times 6} & I_{n\times n}\end{bmatrix} \in \mathbb{R}^{n\times n+6}$ is the matrix selecting the n actuated joints, $\tau \in \mathbb{R}^n$ are the joint torques, $J_c = \frac{\partial c}{\partial q} \in \mathbb{R}^{k\times n+6}$ is the constraint Jacobian, and $f \in \mathbb{R}^k$ are the constraint forces. We now split the constraints into two subsets: the *controlled constraints* (with Jacobian $J_f \in \mathbb{R}^{k_f\times n+6}$ and forces $f_f \in \mathbb{R}^{k_f}$), and the *supporting constraints* (with Jacobian $J_s \in \mathbb{R}^{k_s\times n+6}$ and forces $f_s \in \mathbb{R}^{k_s}$), so that:

$$J_c^T = \begin{bmatrix} J_f^T & J_s^T \end{bmatrix}, \qquad f^T = \begin{bmatrix} f_f^T & f_s^T \end{bmatrix}$$

The problem of regulating f_f to a desired value f_f^* may be formulated as:

$$\begin{aligned} \tau^* = \operatorname*{argmin}_{\tau\in\mathbb{R}^n} & \, ||f_f - f_f^*||^2 \\ s.t. \quad & M\ddot{q} + h - J_s^T f_s - J_f^T f_f = S^T\tau \\ & J_c\ddot{q} = -\dot{J}_c\dot{q}, \end{aligned} \tag{2}$$

where we obtained the second equality constraint by deriving twice the rigid contact constraints $c(q) = 0$ with respect to time. We say that a mechanical system is *sufficiently constrained* if it is subject to enough constraints to satisfy this condition:

$$\text{rank}(J_s U^T) = 6, \tag{3}$$

where $U = \begin{bmatrix} I_{6\times 6} & O_{6\times n}\end{bmatrix}$. If this condition is satisfied, the infinite solutions of the control problem (2) can be expressed as:

$$\begin{aligned} \tau^* &= (N_s S^T)^+ N_s (M\ddot{q}^* + h - J_f^T f_f^*) \\ \ddot{q}^* &= (-J_c^+ \dot{J}_c \dot{q} + N_c \ddot{q}_0), \end{aligned} \tag{4}$$

where $N_s = I - J_s^+ J_s$, $N_c = I - J_c^+ J_c$, and $\ddot{q}_0 \in \mathbb{R}^{n+6}$ is an arbitrary joint acceleration vector. Note that this expression does not contain the constraint forces (i.e. f_s and f_f), so we do not need to measure them. For conciseness we do not report here the derivation of the solution, which can be found in the appendix of [4].

[1] The derivation can be easily extended to deal with nonholonomic constraints too, but for conciseness we restrict the discussion here to holonomic constraints.

B. Comments

The condition (3) has been erroneously approximated in previous works with the less strict condition: $\text{rank}(J_s) \geq 6$. Actually it is true that (3) implies that $\text{rank}(J_s) \geq 6$, but not the opposite — for instance a point-foot quadruped with two feet on the ground verifies the second condition, but not the first one. The intuitive reason why we need at least 6 independent constraint forces that we are willing not to control is that these constraints compensate for the 6 degrees of underactuation of the system. In the constraint-consistent space the system is then fully-actuated, because *the constraint forces can accelerate the virtual base joints in any direction*. In practice, a humanoid robot standing with (at least) one flat foot on the ground always satisfies this condition — in fact we can see it as a fixed-base manipulator. This allows us to feedback-linearize the system and decouple kinematics and dynamics: in (4) we first compute the desired joint accelerations that satisfy the rigid contact constraints $\ddot{q}^*$, and then we use the robot dynamics to compute the corresponding joint torques τ^*. Thanks to this decoupling we can efficiently compute (4) without explicitly calculating the mass matrix M, using the Recursive Newton-Euler Algorithm [6].

When the robot is not *sufficiently constrained* (i.e. (3) is not satisfied), we can still solve the control problem (2), but the resulting control law is more complex and less efficient to compute. Since at the moment our interest lies in cases in which (3) is satisfied, we do not report here this control law. The interested reader can find it in [4].

C. Hierarchical Control

The control law (4) clearly expresses the redundancy of the force task — at kinematic level — with the nullspace term $\ddot{q}_0$, which we can use to perform secondary tasks. Consider the general case in which the robot, besides controlling the constraint forces f_f, has to perform also $N-1$ motion tasks. The force control task has highest priority, because it is a physical constraint that cannot be violated by definition. The motion task i is defined by a Jacobian J_i and a reference acceleration $\ddot{x}_i^*$. The control torques can be computed as:

$$\begin{aligned} \tau^* &= (N_s^T S^T)^+ N_s^T (M\ddot{q}_1 + h - J_f^T f_f^*) \\ \ddot{q}_i &= \ddot{q}_{i+1} + (J_i N_{p(i)})^+ (\ddot{x}_i^* - \dot{J}_i\dot{q} - J_i\ddot{q}_{i+1}) \qquad \forall i \in [1, N] \\ N_{p(i)} &= N_{p(i+1)} - (J_{i+1}N_{p(i+1)})^+ J_{i+1} N_{p(i+1)}, \end{aligned} \tag{5}$$

where $J_N = J_c$, $N_{p(N)} = I$, $\ddot{x}_N^* = 0$ and $\ddot{q}_{N+1} = 0$. Kinematics and dynamics are still decoupled, so τ^* can be efficiently computed with the Recursive Newton-Euler Algorithm [6].

D. Constraint Force Optimization

When the number of supporting constraints is greater than six (i.e. $\text{rank}(J_s) > 6$), there are infinite joint torques τ^* that generate the same controlled forces f_f^* and joint accelerations $\ddot{q}_1$:

$$\begin{aligned} \tau^* &= (N_s^T S^T)_W^+ N_s^T \tau_1 + (I - (N_s^T S^T)_W^+ N_s^T S^T)\tau_0 \\ \tau_1 &= M\ddot{q}_1 + h - J_f^T f_f^*, \end{aligned}$$

where $(N_s^T S^T)_W^+ = W^{\frac{1}{2}}(N_s^T S^T W^{\frac{1}{2}})^+$ is a weighted pseudoinverse, $W \in \mathbb{R}^{n\times n}$ is an arbitrary positive-definite weight matrix and $\tau_0 \in \mathbb{R}^n$ is an arbitrary vector. Changing W and τ_0 we generate different supporting forces f_s. Using (5) we select the minimum norm joint torques that solve the specified control problem. Even if we do not want to control the supporting forces f_f, we may exploit this redundancy to optimize them according to some criteria. Following the approach of Righetti et al. [12], we can minimize the cost $||f_s^T W_f^{-1} f_f||$ by setting:

$$\begin{aligned} W &= (S(J_s^+ W_f^{-1} J_s^{T+} + N_s)S^T)^{-1} \\ \tau_0 &= WS(J_s^+ W_f^{-1} J_s^{T+} + N_s)(M\ddot{q}_1 + h - J_f^T f_f^*) \end{aligned} \tag{6}$$

During the tests we found that this optimization was fundamental to minimize the moments and the tangential forces at the feet in double support phase.

III. Tests

This section presents two simulation tests that validate our control framework while demonstrating its potential and benefits. The first test shows a humanoid robot balancing on its feet (see Fig. 1), while applying a controlled force with its right-arm end-effector on a rigid wall. In the second test the humanoid robot performs a static step with its right foot (see Fig. 2). This test compares the results obtained by the presented controller with the results obtained using the previous approach [11], which does not allow to control forces.

We tested our approach on a customized version of the Compliant huManoid (CoMan) simulator [2]. The robot has 23 joints: 4 in each arm, 3 in the torso and 6 in each leg. Direct and inverse dynamics were computed with C functions, generated by the dynamic engine Robotran [17]. Contact forces were simulated using linear spring-damper models (stiffness $2 \cdot 10^5 N/m$ and damping $10^3 Ns/m$, as proposed in [2]) with realistic friction. To integrate the equations of motion we used the Simulink variable step integrator *ode23t*, with a relative tolerance of 10^{-3} and absolute tolerance of 10^{-6}. The period of the control loop was 1 ms, and the tests were executed on a computer with a 2.83 GHz CPU and 4 GB of RAM.

A. Trajectory Generation

Since the presented control framework works at acceleration level, a drift is likely to occur. To prevent deviations from the desired trajectory and to ensure disturbance rejection, we computed the desired task accelerations $\ddot{x}^* \in \mathbb{R}^m$ with a proportional-derivative feedback control law:

$$\ddot{x}^* = \ddot{x}_r + K_d(\dot{x}_r - \dot{x}) + K_p(x_r - x),$$

where $x_r(t), \dot{x}_r(t), \ddot{x}_r(t) \in \mathbb{R}^m$ are the position-velocity-acceleration reference trajectories, whereas $K_d \in \mathbb{S}_+^m$ and $K_p \in \mathbb{S}_+^m$ are the derivative and proportional gain matrices, respectively. To generate $x_r(t), \dot{x}_r(t), \ddot{x}_r(t)$ we used the approach presented in [10], which provides approximately minimum-jerk trajectories. The trajectory generator is a third order dynamical system that takes as input the desired trajectory $x_d(t)$ and outputs $x_r(t), \dot{x}_r(t), \ddot{x}_r(t)$. The reference position trajectory follows the desired position trajectory with a velocity that depends on the parameter "trajectory time" (between 1 s and 4 s in our tests). We set all the proportional gains $K_p = 10s^{-2}$, and all the derivative gains $K_d = 5s^{-1}$.

B. Test 1 - Multi-contact force control

In this test the robot made contact with a rigid wall using its right hand (see Fig. 1), and it regulated the contact force along the wall normal direction to 20 N. The contact forces at the feet were considered as constraint forces, so they were not controlled. After making contact, we shifted the desired position of the COM towards the right foot of the robot (i.e. along the y direction), so that the robot leaned against the wall, exploiting the additional support provided by the contact on its hand. We report here the overall control hierarchy, in priority order:

- constraints, both feet (12 DoFs);
- force control, right hand (1 DoF);
- position control, COM ground projection (2 DoFs);
- position control, joint posture (29 DoFs).

The RMSE for the force task was about 0.01 N, while for the COM task it was about 0.6 mm. This kind of behavior is extremely difficult to achieve with previous techniques, because they were mainly designed for locomotion tasks and so they do not allow to directly control interaction forces.

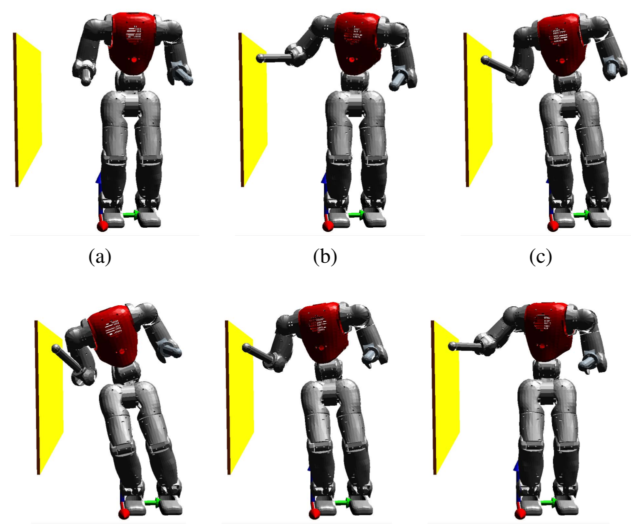

(a) (b) (c) (d) (e) (f)

Fig. 1: Test 1. The robot made contact on the yellow wall; then it moved its COM towards the wall and back.

C. Test 2 - Static walking

This test tackles the switching between different constraint phases, which for instance occurs when switching from single to double support during walking (see Fig. 2). These hard constraint switches cause discontinuities in the control action, which may result in jerky motion or instability. We show how partial force control can eliminate these discontinuities.

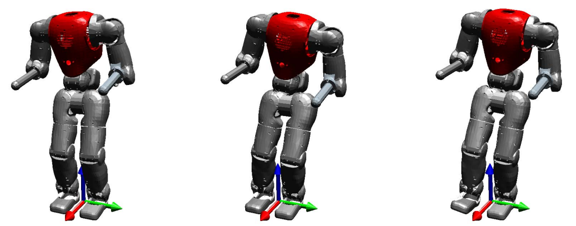

(a) 0 s: COM in the middle.

(b) 2 s: COM over left foot, about to lift right foot.

(c) 3 s: stepping forward.

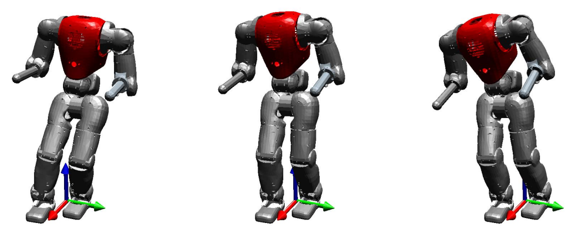

(d) 4 s: ground impact.

(e) 6 s: COM in the middle.

(f) 8 s: COM over right foot.

Fig. 2: Test 2. The robot performing a step with its right foot.

The key idea is to control the forces associated to the constraints that are about to be added to/removed from the constraint set. Namely, before lifting the right foot off the ground, we regulate its contact force to zero, while moving the COM over the left foot. Similarly, when the right foot impacts the ground, we make its contact force slowly raise from zero to an appropriate value (i.e. the weight of the robot), while moving the COM over the right foot. Table I describes the test in terms of which tasks/constraints were active and briefly summarizes each task reference. To stress the benefits of the proposed approach we performed the same test without controlling the contact forces exerted by the right foot on the ground. Table II reports the timeline of this second test. In this case we had to reintroduce the constraints on the right foot before 6 s (i.e. at 5 s) because at 5.5 s the robot could no longer balance due to the lack of force on the right foot.

TABLE I: Timeline of Test 2 using partial force control.

Task	$0-2s$	$2-4s$	$4-6s$	$6-8s$
Constraints	Left foot	Left foot	Left foot	Both feet
Right foot wrench	Decrease		Increase	
COM	Move left	Stay still	Move right	Move right
Right foot pose		Move forward		

TABLE II: Timeline of Test 2 without using partial force control.

Task	$0-2s$	$2-4s$	$4-5s$	$5-8s$
Constraints	Both feet	Left foot	Left foot	Both feet
COM	Move left	Stay still	Move right	Move right
Right foot pose		Move forward		

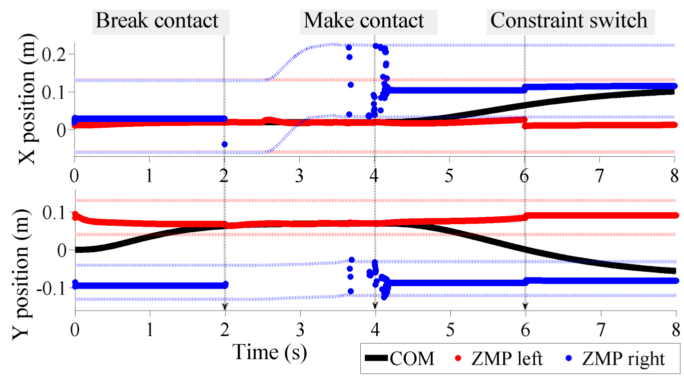

(a) COM and ZMP trajectories during walking with partial force control.

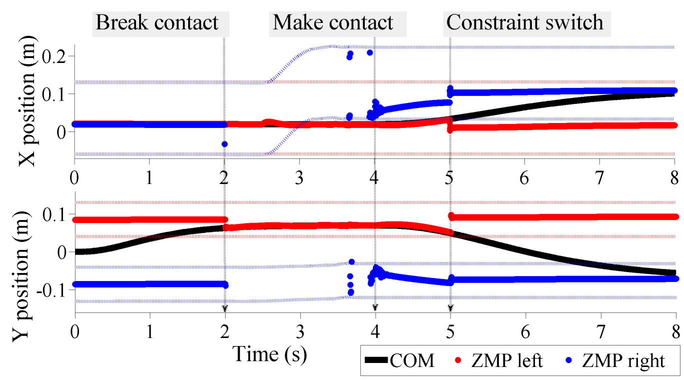

(b) COM and ZMP trajectories during walking without partial force control.

Fig. 3: Test 2. Zero moment point[16] and COM of the robot's feet during static walking. The dotted lines represent the foot borders. At 2 s the robot lifts the right foot off the ground. Right before 4 s the right foot makes contact with the ground. At 6 s the number of constraints changes from 6 to 12.

Whenever there were more than six constraints (i.e. during double support phase), we used the technique described in Section II-D to minimize the moments and the tangential forces at the feet. In particular, we have set the weight matrix $W_f^{-1} \in \mathbb{R}^{12\times 12}$ to a diagonal matrix with entries $\begin{bmatrix} w_l * f_R^{-1} & w_l * f_L^{-1}\end{bmatrix}$, where $w_l = \begin{bmatrix}10 & 10 & 0.1 & 10^3 & 10^3 & 10^2\end{bmatrix}$, and f_R, f_L are the absolute values of the normal forces at the right and left foot, respectively. In this way we penalized the tangential moments the most, followed by the normal moments and the tangential forces. Moreover, we penalized more forces and moments at the foot on which the normal force was lower. This was fundamental to maintain the ZMP[16] inside the foot surface, especially when moving the center of mass away from the central position.

Fig. 3 shows that, when controlling the right foot force, there is almost no discontinuity in the foot ZMPs [16] when breaking the contact (i.e. 2 s) and at the switch of the number of constraints(i.e. 6 s). On the contrary, when not controlling the foot force, we can see a large discontinuity in the ZMP

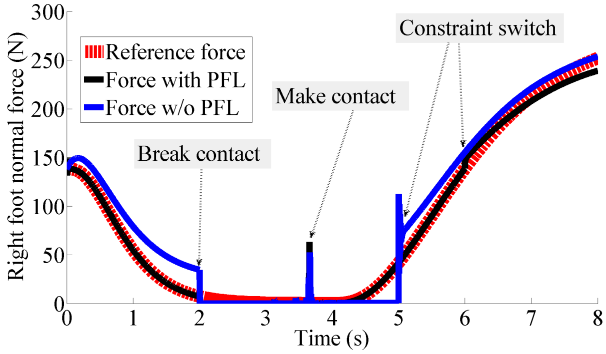

Fig. 4: Test 2. Comparison of the normal contact force at the right foot when walking with/without using Partial Force Control. At 2 s the robot lifts the right foot off the ground. Right before 4 s the right foot makes contact with the ground. At 5 s and 6 s the number of constraints changes from 6 to 12.

of the left foot at 2 s and 5 s. Fig. 4 stresses the different normal contact forces at the right foot, obtained using the two approaches. The force trajectory is almost continuous when using partial force control, whereas there are large discontinuities at 2 s and 5 s when projecting the dynamics in the nullspace of the constraints. The force discontinuity at the impact (right before 4 s) is independent of the control law and it is due to the fact that the foot impacts the ground with nonzero velocity.

IV. Conclusions

We presented a new control law for force control of constrained floating-base mechanical systems. We extended the technique of constraint nullspace projection, to include the control of a subset of the constraint forces exerted by the robot. The presented approach is extremely useful for locomotion control because it allows to drastically reduce the discontinuities in the joint torques and the contact forces. Previous methods overlooked the problem of discontinuities of the contact constraints, even if this can result in jerky movements or instability. Controlling the forces generated by the changing constraints (i.e. constraints that are about to be added to/removed from the constraint set) we can ensure smooth transitions between the different supporting phases of walking. Besides, this control law is fundamental to move beyond simple locomotion tasks, because it allows robots to interact with the environment with their upper body, while balancing or walking.

In this paper we focused on the case in which robots are *sufficiently constrained*, namely the uncontrolled constraint forces can accelerate the virtual base joints in any direction. In practice this condition is often satisfied; for instance humanoids are sufficiently constrained if they have at least one foot in flat contact with the ground. In case the system is not sufficiently constrained it is still possible to find a solution to the studied control problem, but this was outside the scope of this work (the interested reader is referred to [4] for further details). We showed that, for sufficiently constrained systems, the control law takes a particularly simple form. This results in an efficient computation, which does not require the calculation of the mass matrix (computation time below 1 ms on a 2.83 GHz CPU). We integrated this new control law into a prioritized motion/force control framework, to allow the control of multiple motion and force control tasks with different priorities. Moreover, we extended the framework to minimize a quadratic function of the uncontrolled forces (following the approach proposed by Righetti et al. [12]).

To validate the presented theoretical results we carried out two tests on a simulated humanoid robot. The tests validated our control framework while demonstrating two possible applications. The first test focused on controlling a force exerted with the arm end-effector, while controlling the center of mass to balance. The second test show tackled the task of static walking, making a comparison with the standard constraint nullspace projection technique. The results showed how the discontinuities in the contact forces (and hence the zero moment point) can be almost zeroed by controlling the foot contact forces using our approach.

References

[1] Farhad Aghili. A unified approach for inverse and direct dynamics of constrained multibody systems based on linear projection operator: applications to control and simulation. *Robotics, IEEE Transactions on*, 21(5):834–849, 2005. URL http://ieeexplore.ieee.org/xpls/abs_all.jsp?arnumber=1512343.

[2] Houman Dallali, Mohamad Mosadeghzad, Gustavo A Medrano-Cerda, Nicolas Docquier, Petar Kormushev, Nikos Tsagarakis, Zhibin Li, and Darwin Caldwell. Development of a Dynamic Simulator for a Compliant Humanoid Robot Based on a Symbolic Multibody Approach. In *International Conference on Mechatronics, Vicenza, Italy.*, 2013.

[3] Martin De Lasa and Aaron Hertzmann. Prioritized optimization for task-space control. *2009 IEEE/RSJ International Conference on Intelligent Robots and Systems*, 3 (x):5755–5762, October 2009. doi: 10.1109/IROS.2009.5354341. URL http://ieeexplore.ieee.org/lpdocs/epic03/wrapper.htm?arnumber=5354341.

[4] Andrea Del Prete. *Control of Contact Forces using Whole-Body Force and Tactile Sensors : Theory and Implementation on the iCub Humanoid Robot*. PhD thesis, Istituto Italiano di Tecnologia, 2013.

[5] Adrien Escande, Nicolas Mansard, and PB Wieber. Hierarchical Quadratic Programming Part 1: Fundamental Bases. *projects.laas.fr*, 2013. URL http://projects.laas.fr/gepetto/uploads/Publications/2012_escande_ijrr_part1.pdf.

[6] R Featherstone. *Rigid body dynamics algorithms*, volume 49. Springer Berlin:, 2008.

[7] Oussama Khatib. A unified approach for motion and force control of robot manipulators: The operational

space formulation. *IEEE Journal on Robotics and Automation*, 3(1):43–53, February 1987. ISSN 0882-4967. doi: 10.1109/JRA.1987.1087068. URL http://ieeexplore.ieee.org/lpdocs/epic03/wrapper.htm?arnumber=1087068.

[8] Michael Mistry and Ludovic Righetti. Operational Space Control of Constrained and Underactuated Systems. In *Proceedings of robotics: science and systems*, 2011. URL http://www.disneyresearch.com/research/projects/mistry_rss11_final.pdf.

[9] Jaeheung Park. *Control strategies for robots in contact*. PhD thesis, Stanford, 2006. URL http://citeseerx.ist.psu.edu/viewdoc/download?doi=10.1.1.126.6622&rep=rep1&type=pdf.

[10] Ugo Pattacini, Francesco Nori, Lorenzo Natale, Giorgio Metta, and Giulio Sandini. An experimental evaluation of a novel minimum-jerk cartesian controller for humanoid robots. In *Intelligent Robots and Systems (IROS), 2010 IEEE/RSJ International Conference on*, pages 1668–1674. IEEE, 2010. URL http://ieeexplore.ieee.org/xpls/abs_all.jsp?arnumber=5650851.

[11] Ludovic Righetti, Jonas Buchli, Michael Mistry, and Stefan Schaal. Inverse dynamics control of floating-base robots with external constraints: A unified view. *2011 IEEE International Conference on Robotics and Automation*, pages 1085–1090, May 2011. doi: 10.1109/ICRA.2011.5980156. URL http://ieeexplore.ieee.org/lpdocs/epic03/wrapper.htm?arnumber=5980156.

[12] Ludovic Righetti, Jonas Buchli, Michael Mistry, Mrinal Kalakrishnan, and Stefan Schaal. Optimal distribution of contact forces with inverse dynamics control. *The International Journal of Robotics Research*, (January), January 2013. ISSN 0278-3649. doi: 10.1177/0278364912469821. URL http://ijr.sagepub.com/cgi/doi/10.1177/0278364912469821.

[13] L. Saab, Nicolas Mansard, F. Keith, J-Y. Fourquet, and P. Soueres. Generation of dynamic motion for anthropomorphic systems under prioritized equality and inequality constraints. *2011 IEEE International Conference on Robotics and Automation*, pages 1091–1096, May 2011. doi: 10.1109/ICRA.2011.5980384. URL http://ieeexplore.ieee.org/lpdocs/epic03/wrapper.htm?arnumber=5980384.

[14] Luis Sentis. *Synthesis and control of whole-body behaviors in humanoid systems*. PhD thesis, 2008. URL http://gradworks.umi.com/32/81/3281945.html.

[15] Mark W. Spong. The control of underactuated mechanical systems. *First international conference on mechatronics*, 1994. URL http://www.clemson.edu/ces/crb/ece496/spring2004/GroupA/index_files/C59Spong.pdf.

[16] M Vukobratović and B Borovac. Zero-moment point-thirty five years of its life. *International Journal of Humanoid ...*, 2004. URL http://www.worldscientific.com/doi/abs/10.1142/S0219843604000083.

[17] Robotran webpage. http://www.robotran.be, 2012.